

BCSJ Award Article

Design and Synthesis of Semi-Artificial Myoglobin Possessing DNA-Binding Peptides on Heme Propionates

Seiji Sakamoto and Kazuaki Kudo*

Institute of Industrial Science, The University of Tokyo, 4-6-1 Komaba, Meguro-ku, Tokyo 153-8505

Received May 9, 2005; E-mail: kkudo@iis.u-tokyo.ac.jp

Peptides possessing the DNA-binding capability were successfully introduced into myoglobin by a cofactor-reconstitution strategy. We have designed and synthesized an artificial iron–protoporphyrin IX (heme)–peptide conjugate, Heme(br)$_2$, which has covalently conjugated GCN4 basic region peptides at the heme propionate groups as an artificial DNA-binding site. The peptide Heme(br)$_2$ was inserted into apomyoglobin to give a peptide-conjugated myoglobin, Mb(br)$_2$. The UV–vis and circular dichroism spectra of Mb(br)$_2$ were comparable to those of native myoglobin, suggesting that the heme environment and three-dimensional structure of Mb(br)$_2$ were almost identical to those of native myoglobin. The size exclusion chromatography indicated that the Mb(br)$_2$ existed as a monomeric form in an aqueous solution and interacted with its target DNA sequence [c-AMP responsive element (CRE)]. The fluorescence study also revealed that the Mb(br)$_2$ bound CRE DNA effectively with 1/1 stoichiometry [affinity constant; 8.4 ($\pm$0.8) $\times$ 10^7 M^{-1}]. Additionally, the CRE DNA-binding enhanced the peroxidase-like activity of Mb(br)$_2$, possibly due to the partial structural perturbation around the heme active-site. These results demonstrate that the chemical modification of prosthetic group with functional peptides can provide a new strategy for the design of semi-artificial proteins with engineered function.

Myoglobin (Mb) is a relatively small monomeric hemoprotein containing a noncovalently bound iron–protoporphyrin IX (heme).[1] Although in nature the essential role of Mb is oxygen storage, semi-artificial myoglobins possessing non-natural functions and/or artificial molecular binding sites have been prepared by a reconstitutional method that is the incorporation of an artificial heme having multiple functional groups into apomyoglobin (apo-Mb).[2–4] As a pioneering work, Hamachi et al. reported that the aniline hydroxylase activity of Mb bearing unnatural phenylboronic acids was enhanced by the binding of sugars.[2d] As another example, Hayashi and co-workers applied the reconstitution strategy to create a new molecular recognition site nearby the heme center.[3] They introduced multiple charged groups or hydrophobic units at the two heme-propionates and demonstrated the recognition of small substrates and cytochrome *c* on the protein surface. The reconstitution using a chemically modified cofactor is valuable for the active-site directed incorporation of various functional groups, but the previously reported functionalities were relatively small organic and/or inorganic molecules.[2–4] Recently, Fruk and Niemeyer demonstrated that the DNA conjugation at heme propionates imparted Mb with enhanced peroxidase-like activity.[5] This report suggests that the introduction of biopolymers such as polypeptide, protein, RNA, and DNA may expand the utility of the reconstitutional method. In this regard, we designed a semi-artificial Mb having an amphiphilic peptide on the heme and achieved the introduction of flavin functionality or electron-transfer protein via the hetero-stranded coiled-coil formation of the polypeptides.[6] In this study, we used this strategy to create a specific binding domain toward DNA on the surface of Mb by utilizing basic region (br) peptides of the yeast transcription activator GCN4, whose DNA-binding property has been well studied.[7,8] The molecules that bind to a particular nucleotide have been of considerable interest, since such compounds have potential utility for the design of molecular tools for genomic research and for the development of drugs acting as artificial regulators of transcription and translation. As a preliminary investigation for the purpose, we designed a peptide Heme(br)$_2$ that has covalently conjugated br peptides at the heme propionate groups as an artificial DNA-binding site, and we attempted the reconstitution into apo-Mb to get a semi-artificial Mb, Mb(br)$_2$, possessing a DNA-responsible ability.

Results and Discussion

Peptide Design and Synthesis. As a DNA-binding site, we selected the br peptide of the yeast transcription activator GCN4. The GCN4 is one of the most intensively characterized proteins in a bZip motif family.[7,8] The GCN4 is known to bind a DNA sequence, 5′-ATGACGTCAT-3′ [c-AMP responsive element (CRE)] as a homodimer, which is mediated through a coiled-coil structure in the leucine-zipper domain. It was

Published on the web October 4, 2005; DOI 10.1246/bcsj.78.1749

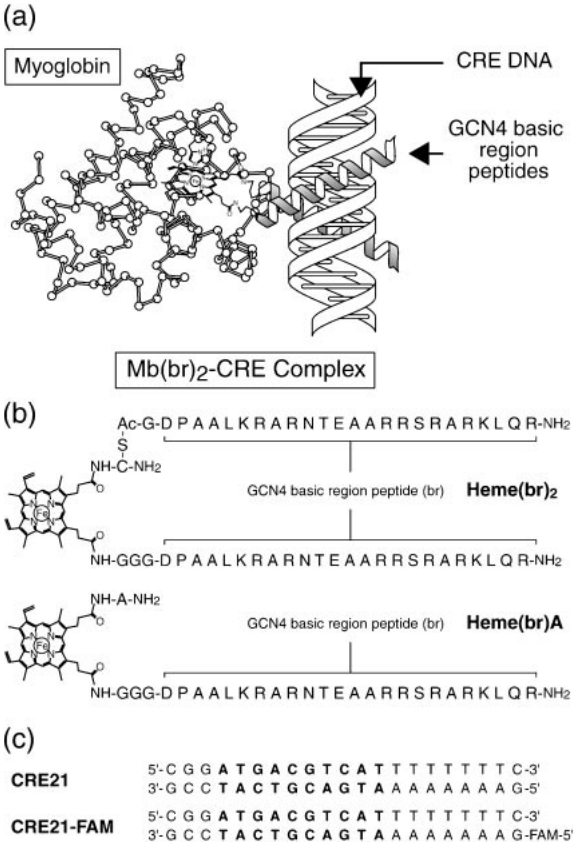

Fig. 1. (a) Schematic illustration of a semi-artificial myoglobin, $Mb(br)_2$, bound to double-stranded DNA. (b) Chemical structure of designed peptides, $Heme(br)_2$ and Heme(br)A. (c) DNA sequence of CRE21 and CRE21-FAM.

found that the GCN4 br peptides dimerized via the disulfide linkage,[9] metal-ion chelation,[10] and other unique linkers[11] were able to bind to their target DNA sequences. On the basis of such information, we designed a peptide-heme conjugate $Heme(br)_2$ in which the 24 mer GCN4 br peptides were conjugated at the ends of heme propionate groups via two flexible spacers, -Gly-Gly-Gly- and -Cys(CH_2CO-Gly-)-NH_2 (Fig. 1). As a control peptide, Heme(br)A, which has only one br segment, was also designed.

The peptides were synthesized by means of both solid-phase and solution methods using the classical Fmoc protocol (Scheme 1).[12] After elongation of H-GGG-br-resin, mono *N*-hydroxysuccinimide ester of protoporphyrin IX was reacted with Gly^1 α-amino group of the peptide on a resin. Then, H-Ala-NH_2 or H-Cys(Trt)-NH_2 was linked to the free propionate group of protoporphyrin IX on solid-phase to produce the intermediates: PPIX(br)A-resin and PPIX(br)C-resin. After cleavage by treatment with trifluoroacetic acid (TFA), the peptide BrAc-br was ligated to the Cys side-chain of PPIX(br)C in 50% trifluoroethanol (TFE)/0.1 M Tris HCl buffer (pH 8.0) ($1\,M = 1\,mol\,dm^{-3}$). After purification of peptides using reversed phase high performance liquid chromatography (RP-HPLC), iron(III) was inserted into the protoporphyrin IX in the peptide by mixing iron(II) acetate in 50% acetic acid (AcOH)/TFE at 50 °C under nitrogen.[13] The heme-peptide

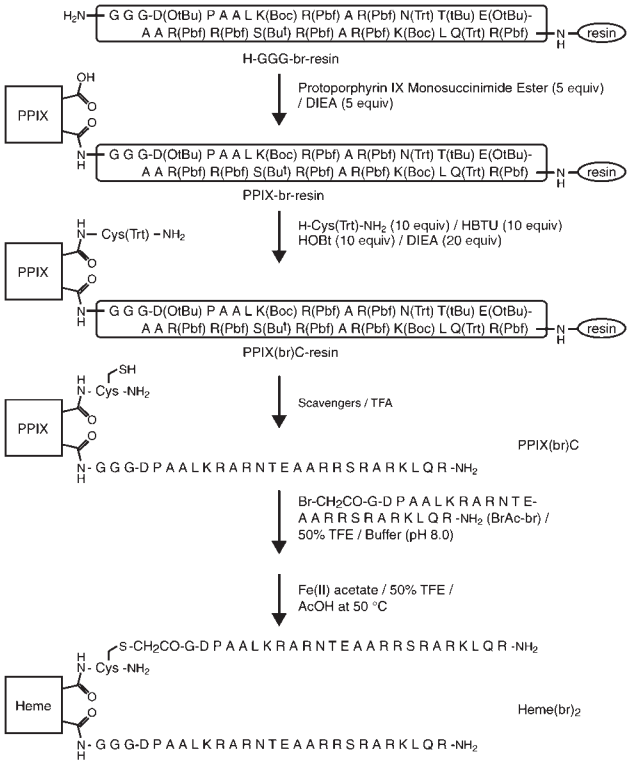

Scheme 1. Synthesis of peptide–heme conjugate, $Heme(br)_2$. The PPIX denotes protoporphyrin IX.

conjugates were purified with RP-HPLC to give a product with high purity (>98%) and were identified by amino acid analysis and matrix-assisted laser desorption ionization time-of-flight mass spectrometry (MALDI-TOFMS) analysis.

Preparation of $Mb(br)_2$ and Mb(br)A. The reconstitution of heme-peptide conjugates with apo-Mb was carried out according to the previously reported method.[2] The stoichiometry of the reconstitution was determined by the titration of the $Heme(br)_2$ with apo-Mb, monitored by using UV–vis spectroscopy, in 20 mM Tris HCl buffer (pH 7.4) containing 2 mM $MgCl_2$, 1 mM ethylenediamine-*N*,*N*,*N*′,*N*′-tetraacetic acid, disodium salt (EDTA 2Na), and 150 mM NaCl. Upon increasing the concentration of apo-Mb, an increase in the Soret band at 408 nm and a decrease of the broad band at around 350 nm were observed in the spectrum (Fig. 2a). The plot of absorbance change at the Soret band as a function of apo-Mb concentration showed the beginning of a plateau at the ratio of [apo-Mb]/[$Heme(br)_2$] = 1/1, suggesting that apo-Mb bound the $Heme(br)_2$ with 1/1 stoichiometry to give a semi-artificial Mb. The reconstituted $Mb(br)_2$ showed absorption maxima at 408 nm (sharp Soret band), 501 nm [β-band (Q_v)], 540 nm [α-band (Q_O)], and 628 nm (π-iron charge transfer band), which are almost coincident with the values of the native Mb under the experimental conditions (Table 1). Upon the addition of an azide or fluoride anion, the 6th ligand of the heme iron in met-Mb is readily exchanged from water to the anion, and the spectroscopic properties under the ligand-binding are useful for probing the heme environment of Mb. In every case, $Mb(br)_2$ showed a spectrum similar to that of native Mb (λ_{max}, fluoride form; 406, 489, and 605 nm: azide form; 420, 542, and 575 nm) [Fig. 2b and Table 1]. A deoxy-$Mb(br)_2$

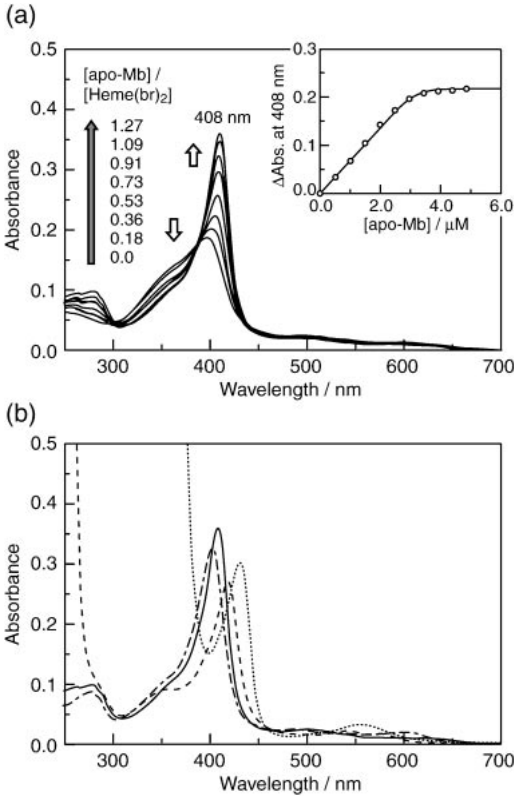

Fig. 2. (a) UV–vis spectra of Heme(br)$_2$ with increasing concentration of apo-Mb in 20 mM Tris HCl/150 mM NaCl/2 mM $MgCl_2$/1 mM EDTA 2Na buffer (pH 7.4) at 25 °C. [Heme(br)$_2$] = 3.0 μM. Inset: plot of absorbance change at 408 nm as a function of apo-Mb concentration. (b) UV–vis spectra of Mb(br)$_2$ in met form (——), N_3^- form (– – –), F^- form (- - - -), and deoxy-form (·····) in a buffer (pH 7.4) at 25 °C. [Mb(br)$_2$] = 3.0 μM.

Table 1. Wavelength of the Peak Maximum in the UV–vis Spectra of Mb(br)$_2$, Mb(br)A, and Native Mb in a Buffer

Conditions	Protein	Peak top of Soret band /nm (ε/M^{-1} cm^{-1})	Peak tops of Q-bands/nm
met form	Mb(br)$_2$	408 (125000)	501, 540, 628
	Mb(br)A	408 (110000)	500, 540, 625[a)]
	Native Mb	409	504, 540, 634
F^- form[b)]	Mb(br)$_2$	406 (108000)	489, 605
	Mb(br)A	406 (103000)	483, 603
	Native Mb	408	495, 606
N_3^- form[b)]	Mb(br)$_2$	420 (90600)	542, 575
	Mb(br)A	419 (95000)	542, 575
	Native Mb	421	541, 574
Deoxy form	Mb(br)$_2$	434 (100000)	556
	Mb(br)A	434 (99100)	555
	Native Mb	434	556

a) Shoulder. b) The UV–vis spectra of F^- form and N_3^- form were measured by the addition of 30 mM KF and 20 mM NaN_3, respectively.

[iron(II) heme state] was also obtained by adding a minimal amount of sodium dithionite to a solution of met-Mb(br)$_2$ in a buffer (Soret band at 434 nm and Q-band at 556 nm). The control peptide Mb(br)A showed similar UV–vis spectroscopic properties. These UV–vis data suggest that the heme environments of the Mb(br)$_2$ and Mb(br)A are almost identical with that of native Mb.

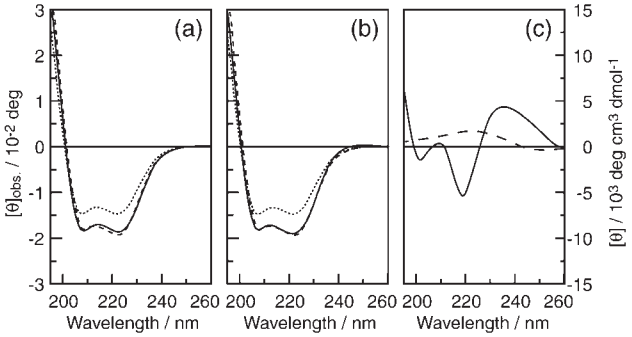

Fig. 3. (a) and (b), CD Spectra of Mb(br)$_2$ (——), Mb (– – –), and apo-Mb (- - - - -) in the absence (a) and presence (b) of CRE21 (1.0 equiv) in a buffer (pH 7.4) at 25 °C. [protein] = 5.0 μM; (c) Difference CD spectra of Mb(br)$_2$ (——) and Mb (- - - - -) obtained by the subtraction of the spectra of protein alone from the spectra of protein and CRE-21 mixture.

Circular Dichroism (CD) Study. The reconstituted Mb(br)$_2$ showed CD spectra with double negative maxima at 208 and 222 nm in a buffer both in the presence and absence of dsDNA containing CRE sequence (CRE21) (Fig. 3). This CD pattern is typical for α-helix dominant proteins and the spectrum is indistinguishable from that of native Mb, suggesting that the artificially introduced br segments do not largely disturb three-dimensional (3D) structure of Mb.[14] The intensity of the negative CD signal at around 220 nm was slightly increased upon addition of CRE21 to Mb(br)$_2$. On the basis of the difference CD spectrum obtained by subtraction of the spectrum of Mb(br)$_2$ alone from the spectrum of Mb(br)$_2$ in the presence of CRE21, the ellipticity change at 222 nm was estimated as -3500 deg cm^2 dmol^{-1} (Fig. 3c). This value is smaller than those of previously reported GCN4 br dimers.[9–11] The binding to a large and negatively charged DNA strand on the Mb surface might partially perturb the protein 3D structure. In contrast to the Mb(br)$_2$, no notable increment in α-helicity of native Mb was observed upon addition of CRE DNA. These results imply that Mb itself cannot interact with CRE and that the increase in α-helicity of Mb(br)$_2$ occurs mainly on the br segments conjugated to the heme propionates. The Mb(br)$_2$ exhibited a positive peak at 406 nm and a negative peak at 360 nm in the absence and presence of CRE21 (Fig. 4). However, the addition of CRE21 significantly weakened the CD intensity at 406 nm. Since the magnitude of CD curves arising from heme in the hemoprotein are sensitive to the protein microenvironment around the heme, the observed result might indicate that the CRE21 binding caused a structural change of heme active site.

Size-Exclusion Chromatography. The interaction between DNA and Mb(br)$_2$ was assessed by size-exclusion chromatography using 5(6)-carboxyfluorescein (FAM) modified CRE21 (CRE21-FAM). In the absence of CRE21-FAM, all proteins showed a single peak on the size-exclusion chromatogram (Figs. 5a–c). A UV–vis spectrum of the peak, measured by photo-diode array system, was indistinguishable from that

of each protein (Figs. 5j–l). This confirmed that the Heme(br)$_2$ and Heme(br)A tightly bound to apo-Mb. The apparent molecular weight ($MW_{app.}$) of each protein, estimated by using natural globular proteins as standards, was almost coincident to the theoretical value (Table 2). This indicates that peptide-conjugated Mb, Mb(br)$_2$, and Mb(br)A as well as native Mb are monomeric forms under the experimental conditions. When the mixture of Mb(br)$_2$ and CRE21-FAM (1.0 equiv) was chromatographed, the peak ascribed to Mb(br)$_2$ decreased and a new peak appeared at a higher molecular weight (elution volume, $V_e = 10.24$ mL) (Fig. 5g). The V_e of the new peak was smaller than that of CRE21-FAM (Fig. 5d) and the UV–vis spectrum of the new peak was identical to that of the Mb(br)$_2$ and CRE21-FAM mixture (Fig. 5m). That is, both Mb(br)$_2$ and CRE21-FAM were co-eluted in the peak, suggesting that the Mb(br)$_2$ and CRE21-FAM bound each other. Moreover, the $MW_{app.}$ of the Mb(br)$_2$/CRE21-FAM complex was almost coincident to the sum of their molecular weights. This implies that Mb(br)$_2$ bound to CRE21-FAM with 1/1 stoichiometry. In contrast, native Mb/CRE21-FAM and Mb(br)A/CRE21-FAM mixtures did not produce a new peak on the chromatogram and each protein was eluted separately (Figs. 5h and j). It is suggested that the two br segments conjugated to heme propionates are necessary to bind CRE DNA tightly in solution.

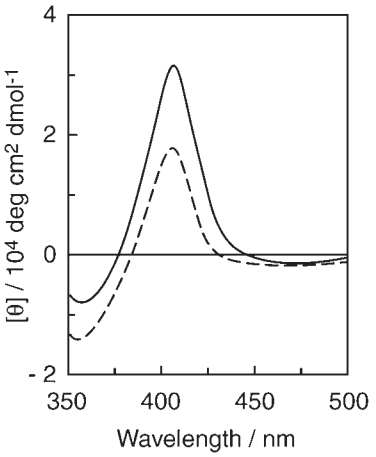

Fig. 4. CD Spectra at the Soret region of Mb(br)$_2$ in the presence (– – –) and absence (——) of CRE21 DNA in a buffer at 25 °C. [protein] = 5 μM.

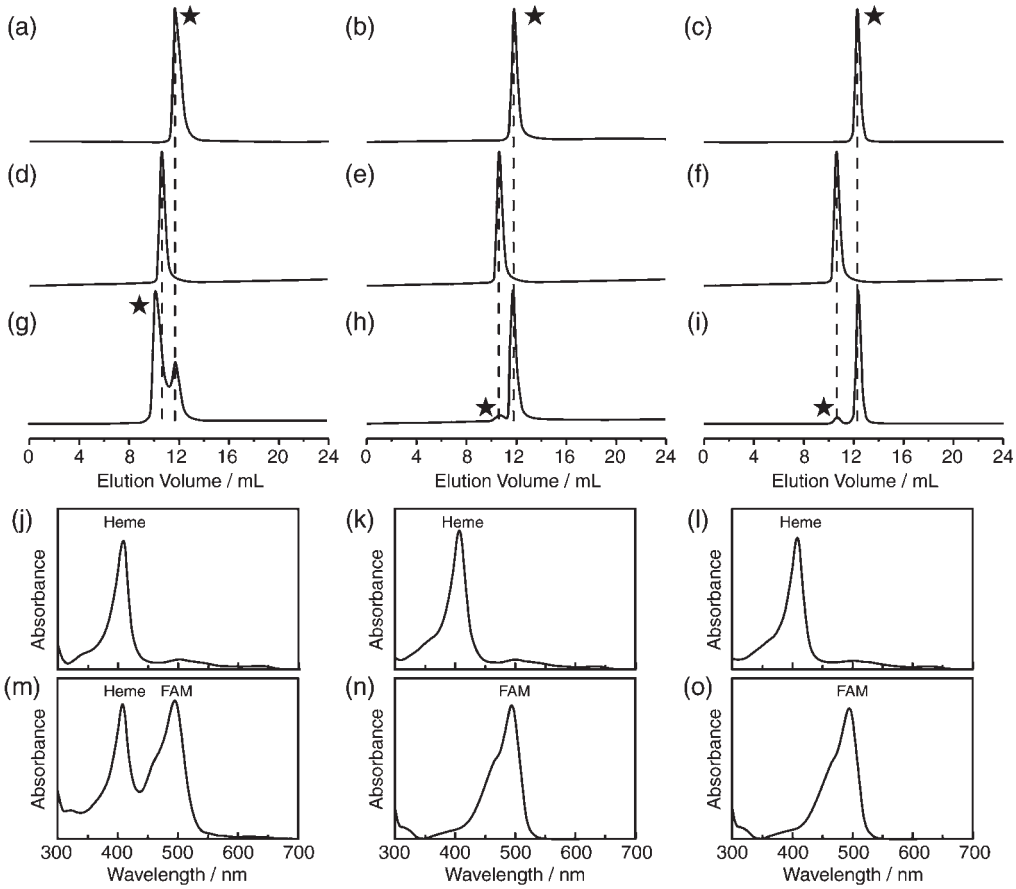

Fig. 5. [(a)–(i)] Size-exclusion chromatograms of Mb(br)$_2$ alone (a), Mb(br)A alone (b), native Mb alone (c), CRE21-FAM alone [(d)–(f)], Mb(br)$_2$/CRE21-FAM mixture (g), Mb(br)A/CRE21-FAM mixture (h), and native Mb/CRE21-FAM mixture (i), detection at 400 nm [(a)–(c) and (g)–(i)] or 500 nm [(d)–(f)]; [protein] = 5 μM and [CRE21-FAM] = 5 μM; Column, Superdex 75HR 10/30 (10 × 300 mm), 20 mM Tris HCl/150 mM NaCl (pH 7.4) at 25 °C; flow rate, 0.4 mL min^{-1}; [(j)–(l)] UV–vis spectra of main peak from Fig. 5(a) [(j)], Fig. 5(b) [(k)], and Fig. 5(c) [(l)]. [(m)–(o)] UV–vis spectra of first eluting peak from Fig. 5(g) [(m)], Fig. 5(h) [(n)], and Fig. 5(i) [(o)]. The peaks giving the spectra were indicated by a star (★). The spectra were measured using Shimadzu SPD10AVP photodiode array UV–vis detector.

Table 2. Apparent Molecular Weight of Protein Estimated by Size-Exclusion Chromatography

Protein	V_e/mL	$MW_{app.}$	MW_{calcd}	$MW_{app.}/MW_{calcd}$
$Mb(br)_2$	11.71	25000	23400	1.07
Mb(br)A	11.80	24100	20510	1.18
$Mb(br)_2$/CRE21-FAM mixture	10.24	43600	36820	1.18
Native Mb	12.32	19900	17500	1.14
apo-Mb	12.22	20660	16940	1.22
CRE21-FAM	10.64	nd[a)]	nd[a)]	nd[a)]

a) Not determined.

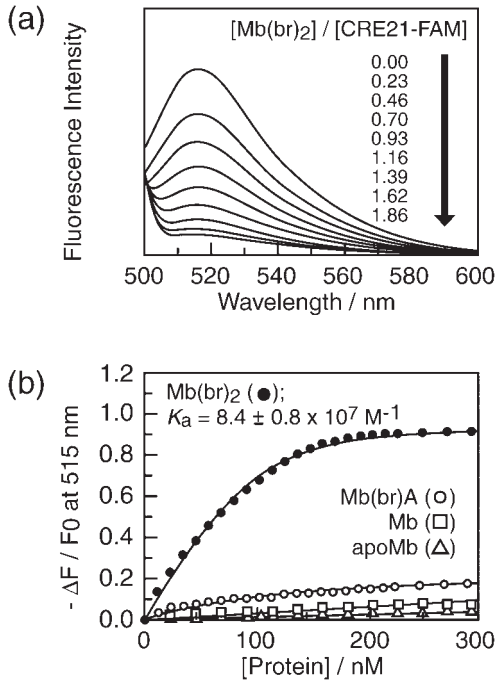

Fig. 6. (a) Fluorescence spectra of CRE21-FAM with increasing concentration of $Mb(br)_2$ in a buffer (pH 7.4) at 25 °C. [CRE21-FAM] = 100 nM. $\lambda_{ex} = 490$ nm. (b) Plots of fluorescence intensity change at 515 nm as a function of $Mb(br)_2$ (●), Mb(br)A (○), Mb (□), and apo-Mb (△) concentration in a buffer (pH 7.4).

Fluorescence Study. The DNA-binding behavior of $Mb(br)_2$ was monitored by fluorescence study using CRE21-FAM. Titration of CRE21-FAM with increasing concentrations of $Mb(br)_2$ gave a concentration-dependent decrease of the fluorescence intensity of FAM at 515 nm (Fig. 6). This result suggests that $Mb(br)_2$ interacts with CRE21-FAM and that the fluorescence of FAM conjugated on DNA is quenched by the amino acid side-chains on Mb, br peptides and/or heme. The affinity constant (K_a) estimated from the change in fluorescence intensity at 515 nm using a single site binding equation was 8.4 ($\pm$0.8) $\times$ 10^7 M^{-1}.[15] The K_a between $Mb(br)_2$ and CRE21-FAM is comparable to those of br peptides dimerized with disulfide bond or other linkers.[8–10] On the other hand, addition of Mb, apo-Mb, and Mb(br)A caused little change in the fluorescence spectra, indicating that these Mb derivatives could not bind CRE DNA sequence effectively under the conditions. The difference between $Mb(br)_2$ and Mb(br)A in the CRE-binding property suggests that the br sequence can act as a dimeric form even on the Mb surface.

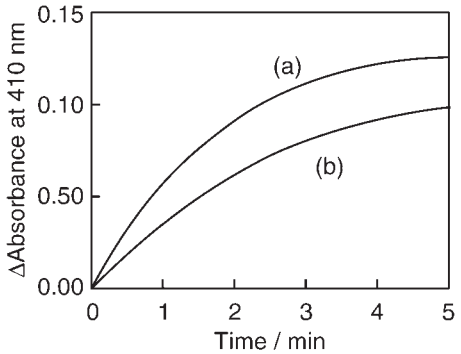

Fig. 7. Time courses of peroxidase-like reaction of $Mb(br)_2$ in the presence (a) and absence (b) of CRE21 DNA (1.0 equiv) in a buffer (pH 7.4) at 25 °C. $[Mb(br)_2] = 1.0$ μM. [ABTS] = 1 mM, and $[H_2O_2] = 0.5$ mM.

Peroxidase-Like Activity of $Mb(br)_2$. Enzymes that show enhanced activity upon binding to a DNA sequence are potentially applicable to a DNA detection system. From this point of view, an $Mb(br)_2$-catalyzed peroxidase-like activity in the presence or absence of CRE21 was investigated using 2,2′-azinobis(3-ethylbenzothiazoline-sulfonic acid) (ABTS) as a substrate and hydrogen peroxide as an oxidant. The oxidation reaction of ABTS is one of the typical reactions catalyzed by peroxidase and could be followed spectrometrically by monitoring the absorbance of the product at 410 nm. The initial rate of $Mb(br)_2$ itself was about 1/3 of that of native Mb under the conditions. However, interestingly, the initial rate of the reaction in the presence of CRE21 was accelerated by a factor of 1.7 compared to that in the absence of CRE21 (Fig. 7). Because the addition of CRE21 gave no effect on the reaction of native Mb, the interactions between the br peptides and CRE DNA play an essential role in the rate enhancement. The enhanced activity cannot be explained by the increased negative charge distribution around the heme active site under the CRE21-binding. The binding of negatively charged DNA nearby the heme periphery seems unsuitable for the access of anionic ABTS substrate. It has been reported that the peroxidase-like catalytic activity of hemoprotein can be enhanced by a small structural change around the heme. For example, Hamachi et al. demonstrated that an electron-transfer protein cytochrome *c* showed the peroxidase-like activity in the presence of lipid bilayers.[16] They suggested the activity of cytochrome *c* was generated by the small conformational conversion around the heme via the bilayer interaction of protein. Possibly, also in our case, the CRE could enhance the activity by binding to the br peptides located on the periphery of the

heme crevice, and by inducing the structural perturbation of active-site to increase the accessibility of ABTS substrate and/or H_2O_2 oxidant.

In conclusion, $Mb(br)_2$, the designed peptide–Mb conjugate, bound CRE, the target DNA strand, with high affinity. The CRE operated as an active effector to regulate the catalytic activity of Mb. Although the acceleration of catalytic rate through the DNA-binding was still too small to use the protein for the detection of a specific DNA sequence, this might be improved through optimization of the mutual distance and the relative orientation between heme and DNA-binding site. Further systematic screening of the functional units and/or the amino acids in the peptide and Mb will lead to the design of artificial protein–DNA assembly on the basis of the *de novo* reconstitutional method. The present strategy using designed peptides conjugated with functional molecules of protein may be applicable to exploration of a new type of functional peptide with extraordinary abilities as sensors and/or artificial enzymes.

Experimental

Materials and Methods. All chemicals and solvents were of reagent or HPLC grade. Protoporphyrin IX and oligo DNA strands were purchased from Sigma-Aldrich Co. Amino acid derivatives and reagents for peptide synthesis were purchased from Novabiochem (Darmstadt, Germany) and Watanabe Chemical Co. (Hiroshima, Japan). All peptides were synthesized manually according to a standard solid-phase method by using Fmoc-strategy.[12] The peptides were purified and analyzed using RP-HPLC on a Cosmosil 5C4-MS semi-preparation column (Nacalai Tesque, Kyoto, Japan) (ϕ 10 × 250 mm) and on a Cosmosil 5C18-AR-II analytical column (ϕ 4.6 × 150 mm) by employing a Shimadzu LC-10ACvp pump equipped with a Shimadzu-SPD10A UV–vis detector and a Shimadzu-CTO-10Avp column oven. MALDI-TOFMS was measured on a Shimadzu MALDI III mass spectrometer by using 3,5-dimethoxy-4-hydroxycinnamic acid as a matrix. Amino acid analysis was carried out after hydrolysis in 6.0 M HCl at 110 °C for 24 h in a sealed tube, and the subsequent labeling with phenyl isothiocyanate. Each peptide concentration was determined by quantitative amino acid analysis using Phe as an internal standard.

Synthesis of BrAc-br, PPIX(br)C, and PPIX(br)A. Peptides PPIX(br)C and PPXI(br)A were precursors of $Heme(br)_2$ and Heme(br)A, respectively, having a free base protoporphyrin IX at the *N*-terminus amino group of the br sequence. A peptide BrAc-br has a bromoacetyl group at the *N*-terminus amino group of the br sequence via Gly spacer. Fmoc-Gly-Gly-Gly-Asp(OBu^t)-Pro-Ala-Ala-Leu-Lys(Boc)-Arg(Pbf)-Ala-Arg(Pbf)-Asn(Trt)-Thr(Bu^t)-Glu(OBu^t)-Ala-Ala-Arg(Pbf)-Arg(Pbf)-Ser(Bu^t)-Arg(Pbf)-Ala-Arg(Pbf)-Lys(Boc)-Leu-Gln(Trt)-Arg(Pbf)-resin (Fmoc-GGG-br-resin) and Fmoc-Gly-Asp(OBu^t)-Pro-Ala-Ala-Leu-Lys(Boc)-Arg(Pbf)-Ala-Arg(Pbf)-Asn(Trt)-Thr(Bu^t)-Glu(OBu^t)-Ala-Ala-Arg(Pbf)-Arg(Pbf)-Ser(Bu^t)-Arg(Pbf)-Ala-Arg(Pbf)-Lys(Boc)-Leu-Gln(Trt)-Arg(Pbf)-resin (Fmoc-G-br-resin) were synthesized by the stepwise elongation of Fmoc-amino acids (Fmoc-AA-OH) on Novasyn TGR resin (Novabiochem) according to a reported procedure with Fmoc-AA-OH [Fmoc-Ala-OH·H_2O, Fmoc-Asn(Trt)-OH, Fmoc-Asp(OBu^t)-OH, Fmoc-Gln(Trt)-OH, Fmoc-Glu(OBu^t)-OH, Fmoc-Gly-OH, Fmoc-Leu-OH, Fmoc-Lys(Boc)-OH, Fmoc-Pro-OH, Fmoc-Ser(Bu^t)-OH, Fmoc-Thr(Bu^t)-OH; Bu^t, *t*-butyl; Boc, *t*-butoxycarbonyl; Trt, trityl] using 2-(1*H*-benzotriazol-1-yl)-1,1,3,3-tetramethyluronium hexafluorophosphate (HBTU), 1-hydroxybenzotriazole hydrate (HOBt·H_2O), and diisopropylethylamine (DIEA) as coupling reagents. Each coupling efficiency was checked by Kaiser test.[17] For the bromoacetylation of *N*-terminus amino group of the BrAc-br, Fmoc-deprotected H-G-br-resin was treated with bromoacetic anhydride (20 equiv) in 1-methyl-2-pyrrolidone (NMP). To introduce protoporphyrin IX moiety at the *N*-terminus amino group of H-GGG-br-resin, we reacted mono *N*-hydroxysuccinimide ester of protoporphyrin IX with Gly^1 α-amino group of the peptide on a resin.[18] Then, H-Ala-NH_2 or H-Cys(Trt)-NH_2 (10 equiv) was coupled on the other propionate group of protoporphyrin IX using HBTU (10 equiv), HOBt·H_2O (10 equiv), and DIEA (20 equiv) as coupling reagents, in order to produce intermediates, PPIX(br)A-resin and PPIX(br)C-resin. The protecting groups and the resin were removed by stirring the dried resin for 2 h at 25 °C with TFA/*m*-cresol/1,2-ethanedithiol/thioanisole (86/6/6/2). The solvent was evaporated and the residues were solidified with diethyl ether on an ice-bath to give crude peptides. Crude peptides were purified with RP-HPLC on a Cosmosil 5C4-MS column (ϕ 10 × 250 mm) using a linear gradient of acetonitrile (MeCN)–0.1% TFA (1.0% min^{-1}) to give the product with a single peak on analytical HPLC [Cosmosil 5C18-AR-II column, ϕ 4.6 × 150 mm with a linear gradient of MeCN–0.1% TFA (1.0% min^{-1})]. The peptides were identified by MALDI-TOFMS; total yield; BrAc-br 8.5%; PPIX(br)C 5.5%; PPIX(br)A 6.0%; MALDI-TOFMS; BrAc-br, m/z 2969.3 [$(M + H)^+$] (calcd = 2970.4); PPIX(br)C, m/z 3609.1 [$(M + H)^+$] (calcd = 3308.6), and PPIX(br)A, m/z 3578.1 [$(M + H)^+$] (calcd = 3576.6).

Synthesis of $PPIX(br)_2$. A peptide $PPIX(br)_2$ was a precursor of $Heme(br)_2$ having a free base protoporphyrin IX. Peptides PPIX(br)C (5 μmol) and BrAc-br (5 μmol) were coupled in 50% TFE/0.1 M Tris HCl (pH 8.0) (2 mL) at 25 °C for 2 h. The crude product was purified with RP-HPLC on a Cosmosil 5C4-MS column (ϕ 10 × 250 mm) using a linear gradient of MeCN–0.1% TFA (1.0% min^{-1}) to give the product with a single peak on analytical HPLC. The peptide was identified by MALDI-TOFMS; yield; 30%; MALDI-TOFMS; m/z 6498.5 [$(M + H)^+$] (calcd = 6497.4).

Synthesis of $Heme(br)_2$ and Heme(br)A. Iron(III) ion was inserted into the protoporphyrin IX group of peptides, $PPIX(br)_2$ and PPIX(br)A by mixing with Fe(II) acetate (20 equiv) in AcOH/TFE (1/1) under nitrogen for 6 h at 50 °C.[12] Crude peptides were purified with RP-HPLC on a Cosmosil 5C4-MS column (ϕ 10 × 250 mm) using a linear gradient of MeCN–0.1% TFA (1.0% min^{-1}) to give the peptides with a single peak on analytical HPLC. The peptides were identified by MALDI-TOFMS and amino acid analysis; yield of $Heme(br)_2$ from $PPIX(br)_2$ 32%, yield of Heme(br)A from PPIX(br)A 31%; MALDI-TOFMS; $Heme(br)_2$ m/z 6573.6 [$(M + Na)^+$] (calcd = 6574.3); Heme(br)A, m/z 3633.5 [$(M + H)^+$] (calcd = 3631.5); Amino acid analysis, obs. (calcd); $Heme(br)_2$ Ala 12.00 (12), Arg 15.6 (14), Asp 3.57 (4), Glu 4.38 (4), Gly 4.84 (4), Leu 3.93 (4), Lys 3.97 (4), Pro 2.12 (2), Ser 2.09 (2), Thr 2.21 (2); Heme(br)A Ala 7.00 (7), Arg 6.68 (7), Asp 1.81 (2), Glu 2.09 (2), Gly 2.83 (2), Leu 1.73 (2), Lys 1.97 (2), Pro 0.89 (1), Ser 0.99 (1), Thr 1.01 (1).

Reconstitution of Semi-Artificial Myoglobin Modified with Peptide. Apomyoglobin was prepared from horse heart myoglobin (Sigma-Aldrich Co.) by the standard method.[19] Peptide–heme conjugates $Heme(br)_2$ and Heme(br)A were incorporated into the heme-binding site of apo-Mb by a slightly modified version of the previously reported procedure.[2] The peptide–heme conjugate (1.5 equiv) dissolved in 50% TFE/20 mM Tris HCl buffer (pH 7.4) was mixed with the solution of apo-Mb in a buffer on an ice bath.

The resulting mixture was incubated at 4 °C overnight. The solution was centrifuged at 4 °C and 10000 rpm for 30 min. The supernatant was passed through a Sephadex G-50 size exclusion column (ϕ 1.0 × 10 cm) in 20 mM Tris HCl buffer (pH 7.4) containing 2 mM $MgCl_2$, 1 mM EDTA 2Na, and 150 mM NaCl, and the fraction containing $Mb(br)_2$ or Mb(br)A was collected and used for analyses without further purifications.

UV–Vis Measurements. UV–vis spectra were recorded on a Shimadzu UV-2200 spectrophotometer using a quartz cell with 1.0 cm pathlength. A heme–peptide conjugate in a buffer was titrated with apo-Mb in increments of about 0.25 equiv. The increase in absorbance at the maximum of the Soret band with increasing apo-Mb concentration was corrected for dilution and the values of the increase were plotted as a function of apo-Mb concentration. For the UV–vis spectrum of deoxy-$Mb(br)_2$ or Mb(br)A, iron(III) in the heme was reduced by the addition of an excess amount of solid sodium dithionite.

Size-Exclusion Chromatography. For analytical size-exclusion HPLC, a Superdex 75HR column (10 × 300 mm) (Pharmacia Biotech.) was used. The chromatographic conditions were as follows; eluent, 150 mM NaCl/20 mM Tris HCl buffer (pH 7.4); flow rate 0.4 mL min^{-1}. The wavelength for the detection was 400 nm (for proteins in the presence and absence of CRE21-FAM DNA) and 500 nm (for CRE21-FAM DNA alone). The spectra of peaks were measured using a Shimadzu SPD10AVP photodiode array UV–vis detector. The protein sample was dissolved in the buffer (5 μM) and 50 μL of the solution was injected. The following proteins were used as standards: bovine serum albumin (67000), ovalbumin (43000), chymotrypsinogen A (25000), and ribonuclease A (13700).

CD Measurements. CD spectra were recorded on a JASCO J-720 spectropolarimeter using a quartz cell with a 1.0 mm pathlength at 25 °C. Proteins were dissolved in 20 mM Tris HCl buffer (pH 7.4) containing 2 mM $MgCl_2$, 1 mM EDTA 2Na, and 150 mM NaCl at a protein concentration of 5 μM.

Fluorescence Measurements. Fluorescence spectra were recorded on a Hitachi 850 fluorescence spectrophotometer with a 1.0 × 1.0 cm quartz cell. A double-stranded CRE21-FAM DNA was dissolved in a buffer (pH 7.4) at a DNA concentration of 100 nM. For the fluorescence titration, CRE21-FAM in a buffer was titrated with a protein in increments of about 0.1 equiv. After each addition of a protein, samples were equilibrated for 10 min at 25 °C; then fluorescence spectra (500–600 nm) excited at 490 nm were measured at 25 °C. The change in fluorescence intensity at 515 nm with increasing protein concentration was corrected for dilution and fitted by a single site binding Eq. 1[15] using Kaleida Graph (Synergy Software) where C_0 and P_0 represent the initial concentration of CRE21-FAM and a protein, respectively.

$$\Delta I/I_0 = \{(\Delta I_{max}/I_0)/2C_0\}[(P_0 + C_0 + 1/K_a) - \{(P_0 + C_0 + 1/K_a)^2 - 4P_0C_0\}^{1/2}]. \quad (1)$$

ΔI denotes the difference in the fluorescence intensity between CRE21-FAM in the absence (I_0) and presence of a protein at each concentration (I). When all the CRE21-FAM bounds to a protein, ΔI is equal to ΔI_{max}.

Assay for ABTS Oxidation. The ABTS oxidation activity of $Mb(br)_2$ was assayed spectrometrically by monitoring the absorbance of the product at 410 nm. The reaction was initiated by the addition of hydrogen peroxide (the final concentration, 0.5 mM) to a mixture of ABTS (substrate) (1 mM), $Mb(br)_2$ (1 μM), and CRE21 (0 or 1 μM) in a buffer (pH 7.4) at 25 °C.

We thank Prof. H. Mihara and Assistant Prof. T. Takahashi (Tokyo Institute of Technology) for MALDI-TOFMS and fluorescence analysis. This work was supported in part by Grants-in-Aid from the Ministry of Education, Culture, Sports, Science and Technology (No. 17710180 for SS).

References

1 E. Antonini and M. Brunori, "Hemoglobin and Myoglobin in Their Reactions with Ligands," North-Holland, Amsterdam (1971).

2 a) Y.-Z. Hu, H. Takashima, S. Tsukiji, S. Shinkai, T. Nagamune, S. Oishi, and I. Hamachi, *Chem.—Eur. J.*, **6**, 1907 (2000). b) Y.-Z. Hu, S. Tsukiji, S. Shinkai, S. Oishi, and I. Hamachi, *J. Am. Chem. Soc.*, **122**, 241 (2000). c) I. Hamachi, T. Matsugi, K. Wakigawa, and S. Shinkai, *Inorg. Chem.*, **37**, 1592 (1998). d) I. Hamachi, Y. Tajiri, T. Nagase, and S. Shinkai, *Chem.—Eur. J.*, **3**, 1025 (1997). e) I. Hamachi, T. Nagase, Y. Tajiri, and S. Shinkai, *J. Chem. Soc., Chem. Commun.*, **1996**, 2205.

3 a) T. Hayashi, T. Matsuda, and Y. Hisaeda, *Chem. Lett.*, **32**, 496 (2003). b) T. Hayashi, H. Dejima, T. Matsuo, H. Sato, D. Murata, and Y. Hisaeda, *J. Am. Chem. Soc.*, **124**, 11226 (2002). c) T. Hayashi, T. Matsuo, Y. Hitomi, K. Okawa, A. Suzuki, Y. Shiro, T. Iizuka, Y. Hisaeda, and H. Ogoshi, *J. Inorg. Biochem.*, **91**, 94 (2002). d) T. Hayashi and Y. Hisaeda, *Acc. Chem. Res.*, **35**, 35 (2002). e) T. Hayashi, Y. Hitomi, T. Ando, T. Mizutani, Y. Hisaeda, S. Kitagawa, and H. Ogoshi, *J. Am. Chem. Soc.*, **121**, 7747 (1999).

4 V. Heleg-Shabtai, T. Gabriel, and I. Willner, *J. Am. Chem. Soc.*, **121**, 3220 (2001).

5 L. Fruk and C. M. Niemeyer, *Angew. Chem., Int. Ed. Engl.*, **44**, 2603 (2005).

6 a) S. Sakamoto, A. Ito, K. Kudo, and S. Yoshikawa, *Chem.—Eur. J.*, **10**, 3717 (2004). b) S. Sakamoto, A. Ito, and K. Kudo, *Chem. Lett.*, **33**, 1202 (2004).

7 T. E. Ellenberger, C. J. Brandl, K. Struhl, and S. C. Harrison, *Cell*, **71**, 1223 (1992).

8 a) M. Suckow, M. Lopata, A. Seydel, B. Kisters-Woike, B. von Wilcken-Bergmann, and B. Muller-Hill, *EMBO J.*, **15**, 598 (1996). b) M. Suckow, K. Schwamborn, B. Kisters-Woike, B. von Wilcken-Bergmann, and B. Muller-Hill, *Nucleic Acids Res.*, **22**, 4395 (1994). c) M. Suckow, A. Madan, B. Kisters-Woike, B. von Wilcken-Bergmann, and B. Muller-Hill, *Nucleic Acids Res.*, **22**, 2198 (1994). d) M. Suckow, B. von Wilcken-Bergmann, and B. Muller-Hill, *Nucleic Acids Res.*, **21**, 2081 (1993).

9 R. V. Talanian, C. J. McKnight, and P. S. Kim, *Science*, **249**, 769 (1990).

10 a) B. Cuenoud and A. Schepartz, *Science*, **259**, 510 (1993). b) C. R. Palmer, L. S. Sloan, J. C. Adrian, Jr., B. Cuenoud, D. N. Paolella, and A. Schepartz, *J. Am. Chem. Soc.*, **117**, 8899 (1995).

11 a) S. Sato, M. Hagihara, K. Sugimoto, and T. Morii, *Chem.—Eur. J.*, **8**, 5067 (2002). b) T. Morii, Y. Saimei, M. Okagami, K. Makino, and Y. Suigiura, *J. Am. Chem. Soc.*, **119**, 3649 (1997). c) M. Ueno, A. Murakami, K. Makino, and T. Morii, *J. Am. Chem. Soc.*, **115**, 12575 (1993).

12 E. Atherton and R. C. Sheppard, "Solid Phase Peptide Synthesis: A Practical Approach," IRL, Oxford, England (1989).

13 F. Nastri, A. Lombardi, G. Morelli, O. Maglio, G. D'Auria, C. Pedone, and V. Pavone, *Chem.—Eur. J.*, **6**, 340 (1997).

14 T. T. Herskovits and N. J. Solli, *Biopolymers*, **14**, 319

(1975).

15 S. Matsumura, S. Sakamoto, A. Ueno, and H. Mihara, *Chem.—Eur. J.*, **6**, 1781 (2000).

16 a) I. Hamachi, A. Fujita, and T. Kunitake, *J. Am. Chem. Soc.*, **119**, 9096 (1997). b) A. Fujita, H. Senzu, T. Kunitake, and I. Hamachi, *Chem. Lett.*, **1994**, 1219.

17 E. Kaiser, R. L. Colescott, C. D. Bossinger, and P. I. Cook, *Anal. Biochem.*, **34**, 595 (1970).

18 I. Obataya, T. Kotaki, S. Sakamoto, A. Ueno, and H. Mihara, *Bioorg. Med. Chem. Lett.*, **10**, 2719 (2000).

19 a) T. Yonetani and T. Asakura, *J. Biol. Chem.*, **244**, 4580 (1969). b) T. Asakura, "Methods in Enzymoogy," ed by S. Fleiser and L. Packer, Academic Press, New York (1978), Vol. 52, Part C, p. 447.